Society of Medical Education & Research

2026, Volume 6, Issue 1, Page No: 103-111
ISSN: 3108-4834

Archive of International Journal of Cancer and Allied Science

Pediatric Cerebellar High-Grade Gliomas Mimic Medulloblastoma Histologically and Transcriptomically but Are Distinct by DNA Methylation Profiling

Noah Williams[1]*, Grace Collins[1], Ethan Brooks[2], Daniel Green[3]

[1]Department of Pediatric Neuro-Oncology and Brain Tumors, Faculty of Medicine, University of Sydney, Sydney, Australia.
[2]Department of DNA Methylation and Tumor Classification, Faculty of Medicine, University of Queensland, Brisbane, Australia.
[3]Department of Cerebellar Glioma and Medulloblastoma Research, Faculty of Medicine, University of New South Wales, Sydney, Australia.

***E-mail** ✉ noah.williams@sydney.edu.au

Abstract

Pediatric high-grade gliomas (HGGs) arising in the cerebellum remain rare, and detailed accounts in the literature are limited. Medulloblastoma constitutes a major differential diagnosis when encountering poorly differentiated tumors in the pediatric cerebellum. The present study delineates the histological and molecular attributes of five cerebellar high-grade gliomas in children. These neoplasms exhibited considerable histological and immunohistochemical overlap with medulloblastomas and registered high scores on a NanoString-based diagnostic assay for medulloblastoma. Epigenetic analysis via methylation profiling revealed heterogeneity, with tumors clustering into the GBM_MID, DMG_K27, and GBM_RTKIII methylation classes. One case harbored MYCN amplification, and two others showed PDGFRA amplification. Targeted sequencing revealed TP53 mutations in all tumors. These observations emphasize that pediatric cerebellar high-grade gliomas can imitate medulloblastomas both morphologically and at the transcriptomic level. This report contributes additional cases to the sparse literature concerning cerebellar HGGs in children. Combined use of methylation array profiling and TP53 screening is recommended when evaluating poorly differentiated cerebellar embryonal-like tumors.

Keywords: Children, High-grade gliomas, p53, PDGFRA, MYCN

Introduction

Brain tumors constitute the most prevalent solid malignancies in children and the foremost cause of mortality from childhood solid cancers [1]. Gliomas account for nearly half of all central nervous system tumors in the pediatric population [2]. While low-grade gliomas predominate among children, high-grade gliomas (HGGs) occur with much lower frequency [3, 4]. Cerebellar high-grade gliomas in children are exceptionally uncommon, representing less than 1% of pediatric brain tumors [3-5].

Most comprehensive series of pediatric high-grade gliomas include few or no cerebellar examples, and their molecular details have rarely been characterized independently from supratentorial counterparts [6-8]. Among 51 pediatric high-grade gliomas in one series, only 1 cerebellar tumor was identified [9]. A broad meta-analysis involving 1069 childhood high-grade gliomas identified merely 21 cerebellar or midline cases [10], with methylation profiling and mutational assessment performed in only five of those [10]. Reinhardt *et al*. [11] examined 86 cerebellar glioblastomas across age groups. Methylation profiling reclassified 25 of these as high-grade astrocytomas with piloid features—a typically

Access this article online https://smerpub.com/

Received: 12 December 2025; **Accepted:** 22 March 2026

How to cite this article: Williams N, Collins G, Brooks E, Green D. Pediatric Cerebellar High-Grade Gliomas Mimic Medulloblastoma Histologically and Transcriptomically but Are Distinct by DNA Methylation Profiling. Arch Int J Cancer Allied Sci. 2026;6(1):103-11. https://doi.org/10.51847/XnqjhrlUbN

circumscribed adult tumor type [12, 13]. Only 13 cases were pediatric [11], of which 5 developed secondary to prior radiotherapy [11]. Mutational data were available for just five of the thirteen pediatric tumors, three of which carried IDH mutations; however, these patients were 15 years or older and aligned with young adult glioma profiles [11]. Buccoliero *et al*. [14] recently reported 11 pediatric high-grade gliomas, including only one cerebellar example. Although anaplastic changes in pilocytic astrocytomas have been documented, the World Health Organization (WHO) Classification (2021) currently regards them as a subtype of pilocytic astrocytoma, which can be difficult to distinguish from high-grade astrocytomas with piloid features [13, 15].

Under the World Health Organization Classification (2021), numerous pediatric-type high-grade gliomas are categorized as IDH-wildtype and H3-wildtype. Korshunov *et al*. [16] further subdivided these into pedGBM_RTK1 (enriched for PDGFRA amplification), pedGBM_RTKII (enriched for EGFR amplification), and pedGBM_MYCN (enriched for MYCN amplification), yet only 4 of 87 cases in their cohort were cerebellar. Thus, cerebellar HGGs in children remain under-studied and poorly characterized.

Given the paucity of information on these rare entities, medulloblastoma emerges as a critical differential diagnosis for poorly differentiated cerebellar tumors in children, as both represent histologically primitive neuroepithelial neoplasms. An archival review across two institutions identified five pediatric cerebellar high-grade gliomas that closely mimicked medulloblastomas on histological examination and also showed transcriptomic similarities. Further evaluation through methylation profiling, bulk RNA sequencing, and targeted sequencing demonstrated clustering with glioma-associated subtypes and the presence of copy number variations (CNVs) typical of glioblastomas. TP53 mutations were detected in all five cases.

Materials and Methods

Patients

Cases were sourced from the pathology archives of the Chinese University of Hong Kong and Huashan Hospital, an affiliated hospital of Fudan University in Shanghai. A systematic review was performed of cerebellar high-grade gliomas and medulloblastomas recorded in the institutional databases from 2002 to 2022 at the Chinese University of Hong Kong and from 2013 to 2022 at Huashan Hospital. The latter facility only commenced routine pediatric admissions in the more recent interval. The tumors included in this analysis — encompassing three lesions originally interpreted as medulloblastomas (as detailed in the Results) — accounted for all identifiable cerebellar high-grade gliomas in children across the study period. In parallel, the two centers performed resections on 192 pediatric medulloblastomas during the corresponding timeframe. Histological evaluation was undertaken independently by two neuropathologists (HKN and HC). Routine laboratory procedures were applied for both histological assessment and immunohistochemical analysis.

Fluorescence In Situ Hybridization (FISH)

Evaluation of BRAF fusion status, MYCN amplification, and PDGFRA amplification relied on FISH analysis. Detection of MYCN alterations employed the BAC clone RP11-355H10, which covers chromosome 2p24 sequences, in combination with the centromeric probe CEP 2 (D2Z1, Vysis). PDGFRA amplification was interrogated using the probes CTD-2054G11 and RP11-231C18, along with the centromeric probe CEP4 (Vysis). For KIAA1549-BRAF fusion, three P1-derived artificial chromosome clones spanning the full BRAF locus (RP4-726N20, RP5-839B19, and RP4-813F11) were paired with the chromosome 7 centromeric enumeration probe CEP7. Spectrum Orange labeling was applied to the target probes, whereas Spectrum Green was used for the reference probes. Scoring and interpretation criteria for FISH followed protocols established in earlier publications from the group [17, 18]. A total of at least 100 non-overlapping nuclei were counted per case. BRAF fusion was judged present when the BRAF/CEP7 ratio was ≥ 1.15 and over 20% of neoplastic cells demonstrated relative gain of BRAF signals [19]. Amplification of MYCN or PDGFRA was recorded if more than 5% of cells exhibited signal clusters or when the target-to-reference probe ratio surpassed 2 [17].

Methylation profiling

Comprehensive genome-wide methylation analysis was executed on DNA derived from FFPE specimens by Sinotech Genomics Co., Ltd. (Shanghai, China), utilizing the workflow previously validated in our laboratory [20]. In outline, extracted DNA underwent bisulfite treatment, restoration, and hybridization to the Illumina Infinium Methylation EPIC 850K BeadChip array. Post-hybridization processing included array washing and

scanning. IDAT file signal intensities received background subtraction and dye-bias correction in accordance with the method of Capper *et al*. [21]. Probes mapping to sex chromosomes and those overlapping known SNPs were omitted. Visualization via t-distributed stochastic neighbor embedding (t-SNE) was achieved with the Rtsne package (version 0.13) as outlined by Capper *et al*. [21]. The processed IDAT files were also submitted to the DKFZ molecular classifier website (www.molecularneuropathology.org, accessed 1 January 2024).

Identification of copy number variations with 850K array

Copy number variation (CNV) profiling followed a strategy comparable to that detailed in our prior work [22]. Concisely, the Bioconductor 'conumee' R package facilitated CNV detection. Amplification or loss was defined by log2-ratio thresholds of ±0.35, while homozygous deletion was set at −0.415 [23].

Target sequencing

Targeted next-generation sequencing was conducted on DNA from FFPE tissues using the approach established earlier [20]. DNA extraction and purification from FFPE material were performed with truXTRAC FFPE Kits (Covaris, Woburn, MA, USA). Sequencing libraries were generated using the KAPA HyperPrep kit (Roche, Cape Town, South Africa) and assessed for quality and concentration before sequencing on the HiSeq platform (Illumina, San Diego, CA, USA). Alignment of paired-end reads was carried out against the hg19 (GRCh37) human reference genome. Variant identification and annotation were performed using smCounter2 and wANNOVAR. Only variants passing quality thresholds, possessing variant allele fractions ≥ 10%, variant allele counts >5, and minor allele frequencies ≤1% in both the 1000 Genomes Project and gnomAD exome datasets were retained for interpretation.

Detection of TERT promoter mutation

Sanger sequencing served to identify TERT promoter mutations, consistent with protocols from previous studies [24, 25]. Crude lysates prepared from FFPE tissue sections served as the template DNA, which was amplified in a PCR mixture containing forward and reverse primers, together with KAPA HiFi HotStart ReadyMix (Roche, Cape Town, South Africa). The primers TERT-F (5′-GTCCTGCCCCTTCACCTT-3′) and TERT-R (5′-CAGCGCTGCCTGAAACTC-3′) amplified a region covering the mutational hotspots C228T and C250T in the TERT promoter. Amplicons were separated by agarose gel electrophoresis, purified, and subjected to cycle sequencing with the BigDye Terminator v1.1 kit (Life Technologies, Carlsbad, CA, USA).

Target RNA sequencing

Total RNA was isolated from FFPE samples using the RNeasy FFPE kit (Qiagen, Hilden, Germany) for targeted RNA sequencing. Following assessment of RNA concentration and integrity, qualifying samples were reverse-transcribed to cDNA. Library construction employed the TruSight RNA Pan-Cancer panel (Illumina), which interrogates 1385 genes implicated in cancer. Alignment of paired-end sequencing reads was performed to the GRCh37 (hg19) human genome assembly. Potential fusion transcripts were identified through the STAR aligner and its associated fusion detection module.

Nanostring-based affiliation

Transcript abundance of 22 medulloblastoma subgroup-defining genes plus three housekeeping genes was quantified using a previously validated NanoString assay [26]. An accompanying R script enabled molecular subgroup classification with an associated confidence metric. This methodology has been widely adopted for determining medulloblastoma subgroups [26, 27]. RNA extraction from FFPE tissue was accomplished with the RNeasy FFPE Kit (Qiagen), followed by spectrophotometric quantification on a NanoDrop 2000 instrument. Hybridization to the NanoString nCounter CodeSet occurred at 67 °C over 20 hours. Post-hybridization processing involved purification and immobilization on cartridges via the nCounter Prep Station (NanoString Technologies, Seattle, WA, USA). Digital readout of fluorescent signals was performed on the nCounter Digital Analyzer (NanoString Technologies). Normalization of raw counts used the 'NanoStringNorm' R package, and subgroup predictions were generated with the 'pamr' package.

Immunohistochemistry

Expression of GFAP, Ki67, Olig2, Synaptophysin, and p53 was evaluated by immunohistochemistry. Four-micrometer FFPE sections were deparaffinized in xylene and rehydrated in a descending ethanol series. Automated staining was carried out on either the BenchMark

ULTRA system (Ventana Medical Systems, Rotkreuz, Switzerland) or the Bond Max platform (Leica Biosystems, Nußloch, Germany). The following antibodies were applied: GFAP (Dako Z0334, 1:2500), Ki67 (Thermo Fisher SP6, 1:200), Olig2 (IBL-America 18953, 1:120), Synaptophysin (Novocastra NCL-L-SYNAP-299, 1:50), and p53 (Dako DO-7, 1:40). Visualization utilized the OptiView DAB IHC Detection Kit (Ventana Medical Systems). Strong nuclear p53 immunoreactivity in > 10% of tumor cells was considered positive [28].

Results and Discussion

Four individuals had highly restricted overall survival (OS), ranging from 5 months to 1 year, and 4 received postoperative adjuvant treatment. The patient with the longest survival was the most recently diagnosed case. Representative magnetic resonance imaging and histopathological findings appear in **Figure 1**. Imaging files for one patient could not be retrieved due to hospital archiving. Radiologically, the tumors in all five cases occupied a relatively central position in the cerebellum rather than a lateral distribution. Tumor epicenters were situated within the cerebellar hemispheres or associated peduncles.

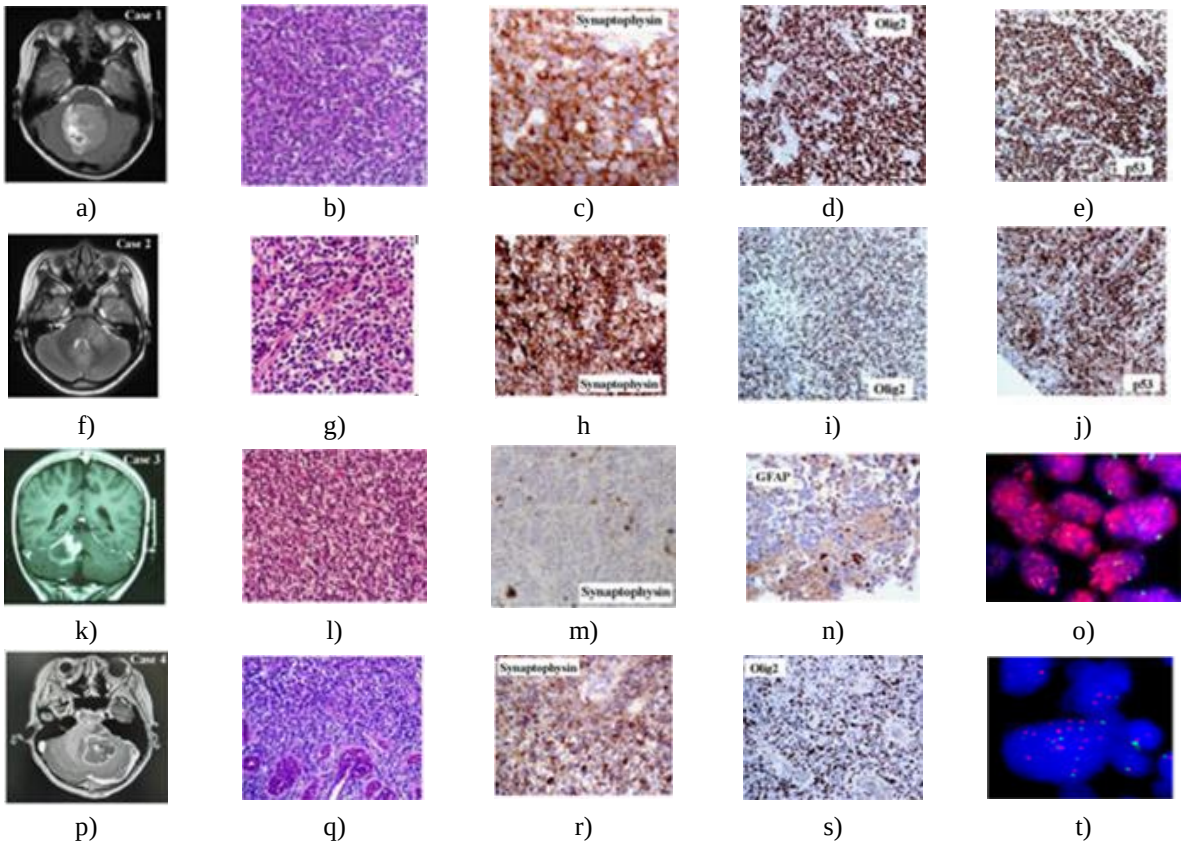

Figure 1. Histological and immunohistochemical profiles of the tumor specimens.

(a–e) Case 1: (a) T2 MRI demonstrating a substantial fourth ventricular mass, (b) H&E stain illustrating sheets of uniform small hyperchromatic cells exhibiting embryonal features and scant cytoplasm (×200). Immunopositivity was observed for (c) synaptophysin (×400), (d) Olig2 (×200), and (e) p53 (×200). Neoplastic cells lacked GFAP and NeuN expression, retained INI-1, and displayed a high Ki67 proliferation index (data not shown). (f–j) Case 2. (f) T2 MRI revealing a large mass involving the cerebellar peduncle and fourth ventricle, (g) H&E stain showing primitive cell sheets comparable to those in Case 1 (×200). Positive staining for (h) synaptophysin (×400), (i) Olig2 (×200), and (j) p53 (×200). The tumor cells were negative for NeuN, focally positive for GFAP, retained INI-1 expression, and exhibited elevated Ki67 labeling (not illustrated). (k–o)

Case 3, (k) T2 MRI indicating a mass at the cerebellar peduncle. Histological examination demonstrated (l) aggregates of hyperchromatic cells with minimal cytoplasm (×200), along with limited necrosis and microvascular proliferation (not shown). Immunoreactivity included (n) synaptophysin (×200) and (m) GFAP (×400). Tumor cells showed focal Olig2 positivity, absence of NeuN, retention of INI-1, p53 expression, and a high Ki67 index (not shown). (o) FISH analysis confirmed PDGFRA amplification in line with CNV data. (p–t) Case 4, (P) T2 MRI displaying a large cerebellar lesion, (q) H&E stain depicting sheets of hyperchromatic embryonal cells with focal microvascular proliferation (×400). Staining was positive for (r) synaptophysin (×400) and (s) Olig2 (×200). Focal p53 and GFAP positivity were noted, with negativity for NeuN, retention of INI-1, and high Ki67 labeling. (t) FISH revealed MYCN gains, concordant with CNV results.

All five tumors exhibited a striking histological similarity to medulloblastomas, manifesting as diffuse, patternless sheets of tightly apposed, monomorphic, primitive cells with hyperchromatic nuclei and minimal cytoplasm. Neither Homer-Wright rosettes nor astrocytic elements such as fibrillary processes or gemistocytes were identified. Nodular growth patterns were absent, and no characteristics of pilocytic astrocytoma were evident. Focal necrosis was present in Cases 3 and 5, while microvascular proliferation occurred in Cases 3 and 4. Immunohistochemistry revealed consistent strong synaptophysin reactivity (focal in one instance) and prominent Olig2 expression (focal in one), alongside inconsistent GFAP staining. Proliferation rates assessed by Ki67 were markedly elevated across the series. Strong nuclear p53 accumulation was detected in most tumors (focal in one) **(Figure 1)**.

NanoString transcriptomic profiling for medulloblastoma molecular subgroup assignment was performed at diagnosis for two cases (#1 and #2), both yielding high confidence scores that assigned them to specific medulloblastoma subgroups **(Figure 2)**. Subsequent testing of two further cases produced successful results, with one attaining a high confidence score **(Figure 2)**. One archival case could not be adequately evaluated by this method. Three tumors, including the two with initial high-confidence NanoString assignments, had been originally classified as medulloblastomas belonging to defined molecular subgroups (Cases 1, 2, and 5). The remaining two tumors received an initial diagnosis of high-grade glioma.

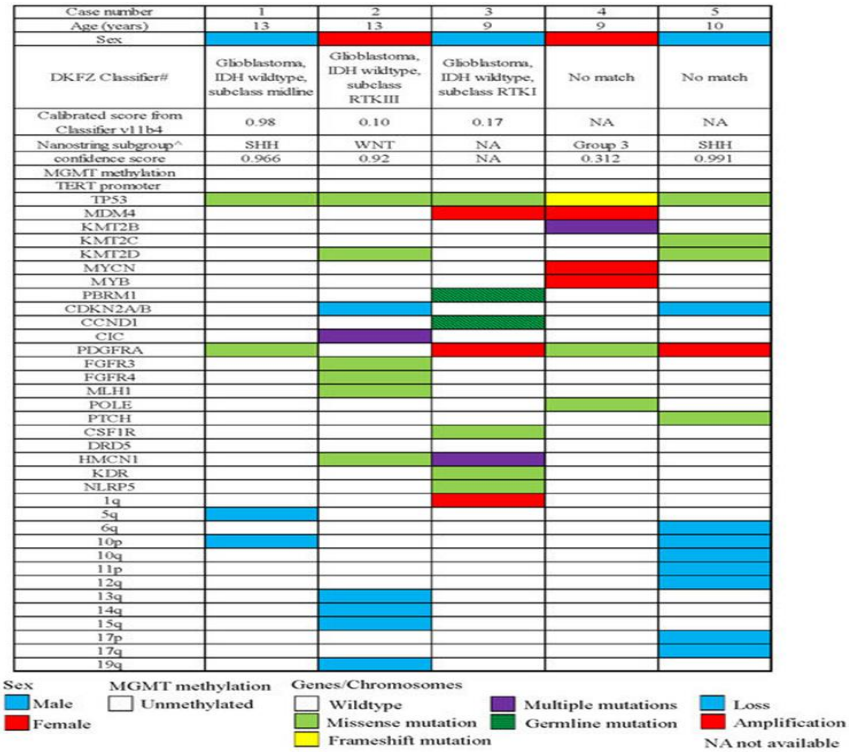

Figure 2. Oncoprint depicting the clinical and molecular features of the series. ^ NanoString transcriptome profiling conducted as reported in earlier publications [26, 27]. # Methylation classification determined via the DKFZ classifier [21].

DNA methylation profiling was retrospectively performed on all cases using Illumina Infinium 850K arrays and positioned within the t-SNE reference landscape of the DKFZ Molecular Neuropathology cohort. In keeping with the classification framework of Capper *et al*. [21], glioblastomas can be epigenetically categorized into GBM RTK II and GBM mesenchymal (MES) groups, with rarer representation of GBM RTK I, GBM RTK III, GBM MID, GBM MYCN, and GBM G34 [29]. Three cases clustered closely to or within the GBM_MID class. One tumor aligned near the DMG_K27 class, while another mapped to the GBM_RTKIII class **(Figure 3)**. CNV profiling based on methylation data detected MYCN amplification in one tumor and PDGFRA amplification in two others **(Figure 2)**. These findings were corroborated by FISH analysis **(Figure 1)**. As referenced in the Introduction, such amplifications of PDGFRA and MYCN are recognized features in subsets of pediatric H3-wildtype high-grade gliomas [16].

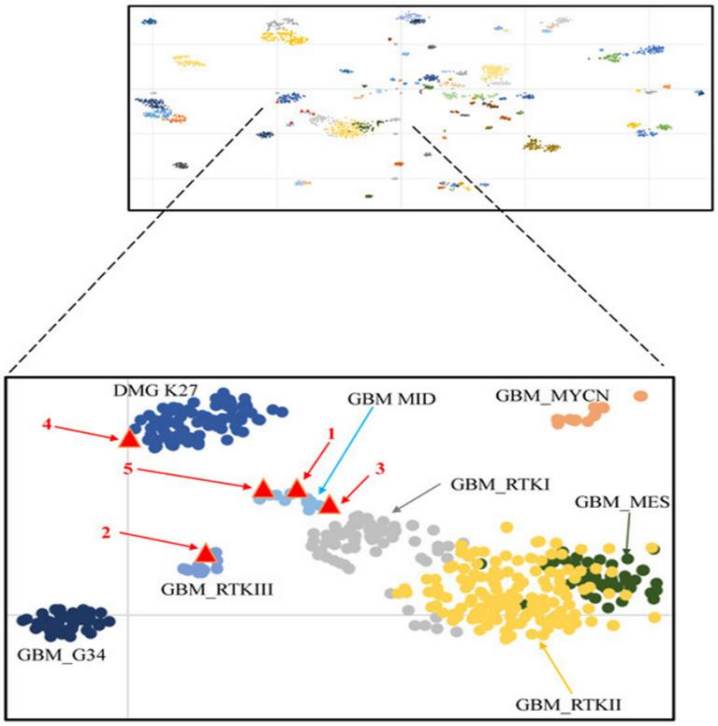

Figure 3. t-SNE visualization of DNA methylation profiles for the five study tumors (red triangles) relative to 2801 reference cases from Capper *et al*. [21].

Targeted DNA panel sequencing was also performed on all five tumors. TP53 mutations were universally present, consisting of four missense changes and one frameshift variant, in agreement with p53 immunohistochemical results **(Figures 1 and 2)**. Recurrent mutations also involved KMT2D and PDGFRA. No alterations were found in H3F3A, HIST1H3B, BRAF, the TERT promoter region, or IDH genes. The absence of H3 mutations was particularly relevant given the central posterior fossa locations, thereby excluding extension from a typical H3K27-mutated diffuse intrinsic pontine glioma (DIPG). Germline analysis in two patients with available blood samples identified PBRM1 (p.D163N) and CCND1 (p.A270V) variants in one case; both were interpreted as variants of uncertain significance according to standard criteria. Germline TP53 mutations were not detected.

Fusion gene screening was performed via RNA sequencing, but insufficient material limited analysis to three cases (Cases 1, 3, and 5), none of which harbored identifiable fusions. FISH testing for BRAF fusion was negative in all cases.

High-grade gliomas of the cerebellum in children occur infrequently, and information on the specific molecular drivers of these neoplasms is correspondingly limited. Large-scale studies of pediatric high-grade gliomas, as referenced in the Introduction, have included only a few cerebellar cases. Findings from this modest series indicate that such uncommon pediatric cerebellar high-grade gliomas frequently share substantial histological, immunohistochemical, and transcriptomic traits with medulloblastomas. In all five instances examined here, the neoplasms consisted of compact sheets of primitive cells displaying hyperchromatic nuclei and minimal cytoplasm, thereby recapitulating the classic appearance of medulloblastoma. Furthermore, diffuse strong synaptophysin expression was evident in all cases, consistent with one of the most widely used diagnostic markers for medulloblastoma in neuropathological assessment [30]. Most differential considerations for medulloblastoma, aside from ETMR, typically lack significant neuronal marker expression, such as synaptophysin [30]. By comparison, positivity for Olig2 or GFAP tends to be confined to sparse cells within true medulloblastomas [30-32]. Necrosis and microvascular proliferation were observed in three tumors in the series; although not pathognomonic for glioblastoma, these features can provide valuable diagnostic clues, especially when evaluated alongside Olig2 staining.

Although the NanoString assay is extensively employed for both diagnosis and molecular stratification of medulloblastomas [27], it is acknowledged that certain non-medulloblastoma entities may occasionally yield misleading results. Korshunov *et al*. [33] reported that, among 239 tumors provisionally assigned to the medulloblastoma category via NanoString, methylation profiling ultimately reclassified 18 cases (8%) as alternative brain tumor types. The examples detailed in the current series confirm that cerebellar high-grade gliomas can generate exceptionally high confidence scores on the NanoString platform for medulloblastoma subgroups, in parallel with their morphological mimicry. These observations strongly endorse methylation profiling as the preferred modality for clarifying the identity of poorly differentiated tumors arising in the pediatric cerebellum.

Every tumor in the cohort harbored TP53 mutations. Such variants are documented in roughly half of non-brainstem pediatric high-grade gliomas and predominate in H3F3A G34V/R gliomas [7]. Given the overall rarity of cerebellar HGGs and the paucity of molecular data highlighted in the Introduction, relevant literature is sparse. Zhang *et al*. [34] performed whole-genome sequencing and/or RNA sequencing on 854 pediatric brain tumors across diverse categories and detected only 4 cerebellar high-grade gliomas, 3 of which harbored TP53 mutations. The fourth case instead featured an NF1 alteration [34]. Likewise, the solitary pediatric cerebellar high-grade glioma described by Buccoliero *et al*. [14] harbored a TP53 mutation as its sole genetic alteration. In a separate cohort of 32 radiation-induced pediatric gliomas, TP53 mutations were detected in 2 of 8 cerebellar high-grade tumors linked to prior irradiation [35]. Of note, TP53 alterations also characterize a prognostically adverse subset of SHH-activated medulloblastomas [36]. Routine p53 immunohistochemistry remains a reliable surrogate for detecting underlying TP53 mutations in clinical practice [37].

Overall, the current investigation delivers a comprehensive histological and genomic profile for a small collection of sporadic pediatric cerebellar high-grade gliomas. These lesions can imitate medulloblastoma at multiple biological levels. The data underscore the value of methylation profiling, in conjunction with conventional diagnostic strategies, as the optimal approach for investigating poorly differentiated pediatric cerebellar tumors.

Conclusion

This analysis contributes to a more refined appreciation of the uncommon pediatric cerebellar high-grade gliomas. The study reveals that these neoplasms may exhibit transcriptomic and morphological overlap with medulloblastomas. In addition to established techniques for separating various embryonal tumors, including atypical teratoid/rhabdoid tumor (ATRT) and embryonal tumor with multilayered rosettes (ETMR), we propose the routine application of methylation profiling when practicable, supplemented by Olig2 and p53 immunohistochemical evaluation, to improve diagnostic precision for poorly differentiated embryonal-like neoplasms in the cerebellum.

Acknowledgments: None

Conflict of Interest: None

Financial Support: None

Ethics Statement: None

References

1. Thorbinson C, Kilday JP. Childhood Malignant Brain Tumors: Balancing the Bench and Bedside. Cancers (Basel). 2021;13(23):6099.
2. Ostrom QT, de Blank PM, Kruchko C, Petersen CM, Liao P, Finlay JL, et al. Alex's Lemonade Stand Foundation Infant and Childhood Primary Brain and Central Nervous System Tumors Diagnosed in the United States in 2007-2011. Neuro Oncol. 2015;16(Suppl 10):x1-36.
3. Ostrom QT, Cioffi G, Waite K, Kruchko C, Barnholtz-Sloan JS. CBTRUS Statistical Report: Primary Brain and Other Central Nervous System Tumors Diagnosed in the United States in 2014-2018. Neuro Oncol. 2021;23(Suppl 3):iii1-105.
4. Sturm D, Pfister SM, Jones DTW. Pediatric Gliomas: Current Concepts on Diagnosis, Biology, and Clinical Management. J Clin Oncol. 2017;35(21):2370-7.
5. Karremann M, Rausche U, Roth D, Kühn A, Pietsch T, Gielen GH, et al. Cerebellar location may predict an unfavourable prognosis in paediatric high-grade glioma. Br J Cancer. 2013;109(4):844-51.
6. Korshunov A, Ryzhova M, Hovestadt V, Bender S, Sturm D, Capper D, et al. Integrated analysis of pediatric glioblastoma reveals a subset of biologically favorable tumors with associated molecular prognostic markers. Acta Neuropathol. 2015;129(5):669-78.
7. Mackay A, Burford A, Molinari V, Jones DTW, Izquierdo E, Brouwer-Visser J, et al. Molecular, Pathological, Radiological, and Immune Profiling of Non-brainstem Pediatric High-Grade Glioma from the HERBY Phase II Randomized Trial. Cancer Cell. 2018;33(5):829-42.e5.
8. Wu G, Diaz AK, Paugh BS, Rankin SL, Ju B, Li Y, et al. The genomic landscape of diffuse intrinsic pontine glioma and pediatric non-brainstem high-grade glioma. Nat Genet. 2014;46(5):444-50.
9. Sturm D, Witt H, Hovestadt V, Khuong-Quang DA, Jones DT, Konermann C, et al. Hotspot mutations in H3F3A and IDH1 define distinct epigenetic and biological subgroups of glioblastoma. Cancer Cell. 2012;22(4):425-37.
10. Mackay A, Burford A, Carvalho D, Izquierdo E, Fazal-Salom J, Taylor KR, et al. Integrated Molecular Meta-Analysis of 1,000 Pediatric High-Grade and Diffuse Intrinsic Pontine Glioma. Cancer Cell. 2017;32(4):520-37.e5.
11. Reinhardt A, Stichel D, Schrimpf D, Koelsche C, Wefers AK, Ebrahimi A, et al. Tumors diagnosed as cerebellar glioblastoma comprise distinct molecular entities. Acta Neuropathol Commun. 2019;7(1):163.
12. Brat DJ, Ellison DW, Figarella-Branger D, Hawkins CE, Louis DN, Perry A, et al. Gliomas, Glioneuronal Tumours, and Neuronal Tumours. In: WHO Classification of Tumours Editorial Board, editor. Central Nervous System Tumours. 5th ed. Lyon: IRAC; 2021. p. 90-2. (WHO Classification of Tumours; vol. 6).
13. Reinhardt A, Stichel D, Schrimpf D, Sahm F, Korshunov A, Reuss DE, et al. Anaplastic astrocytoma with piloid features, a novel molecular class of IDH wildtype glioma with recurrent MAPK pathway, CDKN2A/B and ATRX alterations. Acta Neuropathol. 2018;136(2):273-91.
14. Buccoliero AM, Giunti L, Moscardi S, Castiglione F, Provenzano A, Sardi I, et al. Pediatric High Grade Glioma Classification Criteria and Molecular Features of a Case Series. Genes (Basel). 2022;13(4):624.
15. Gareton A, Tauziède-Espariat A, Dangouloff-Ros V, Roux A, Saffroy R, Castel D, et al. The histomolecular criteria established for adult anaplastic pilocytic astrocytoma are not applicable to the pediatric population. Acta Neuropathol. 2020;139(2):287-303.
16. Korshunov A, Schrimpf D, Ryzhova M, Sturm D, Chavez L, Hovestadt V, et al. H3-/IDH-wild type pediatric glioblastoma is comprised of molecularly and prognostically distinct subtypes with associated oncogenic drivers. Acta Neuropathol. 2017;134(3):507-16.
17. Yang RR, Aibaidula A, Wang WW, Chan AK, Shi ZF, Zhang Z, et al. Pediatric low-grade gliomas can

be molecularly stratified for risk. Acta Neuropathol. 2018;136(4):641-55.
18. Aibaidula A, Chan AK, Shi Z, Li Y, Zhang R, Yang R, et al. Adult IDH wild-type lower-grade gliomas should be further stratified. Neuro Oncol. 2017;19(10):1327-37.
19. Horbinski C, Hamilton RL, Nikiforov Y, Pollack IF. Association of molecular alterations, including BRAF, with biology and outcome in pilocytic astrocytomas. Acta Neuropathol. 2010;119(5):641-9.
20. Liu EM, Shi ZF, Li KK, Malta TM, Chung NY, Chen H, et al. Molecular landscape of IDH-wild type, pTERT-wild type adult glioblastomas. Brain Pathol. 2022;32(5):e13107.
21. Capper D, Jones DTW, Sill M, Hovestadt V, Schrimpf D, Sturm D, et al. DNA methylation-based classification of central nervous system tumours. Nature. 2018;555(7697):469-74.
22. Wong QH, Li KK, Wang WW, Malta TM, Noushmehr H, Grabovska Y, et al. Molecular landscape of IDH-mutant primary astrocytoma Grade IV/glioblastomas. Mod Pathol. 2021;34(7):1245-60.
23. Shirahata M, Ono T, Stichel D, Schrimpf D, Reuss DE, Sahm F, et al. Novel, improved grading system(s) for IDH-mutant astrocytic gliomas. Acta Neuropathol. 2018;136(1):153-66.
24. Chan AK, Yao Y, Zhang Z, Chung NY, Liu JS, Li KK, et al. TERT promoter mutations contribute to subset prognostication of lower-grade gliomas. Mod Pathol. 2015;28(2):177-86.
25. Ng HK, Li KK, Chung NY, Chan JY, Poon MF, Wong QH, et al. Molecular landscapes of longitudinal NF2/22q and non-NF2/22q meningiomas show different life histories. Brain Pathol. 2023;33(2):e13120.
26. Wong GC, Li KK, Wang WW, Liu AP, Huang QJ, Chan AK, et al. Clinical and mutational profiles of adult medulloblastoma groups. Acta Neuropathol Commun. 2020;8(1):191.
27. Northcott PA, Shih DJ, Remke M, Cho YJ, Kool M, Hawkins C, et al. Rapid, reliable, and reproducible molecular sub-grouping of clinical medulloblastoma samples. Acta Neuropathol. 2012;123(4):615-26.
28. Takami H, Yoshida A, Fukushima S, Arita H, Matsushita Y, Nakamura T, et al. Revisiting TP53 Mutations and Immunohistochemistry--A Comparative Study in 157 Diffuse Gliomas. Brain Pathol. 2015;25(3):256-65.
29. Stichel D, Ebrahimi A, Reuss D, Schrimpf D, Ono T, Shirahata M, et al. Distribution of EGFR amplification, combined chromosome 7 gain and chromosome 10 loss, and TERT promoter mutation in brain tumors and their potential for the reclassification of IDHwt astrocytoma to glioblastoma. Acta Neuropathol. 2018;136(5):793-803.
30. Orr BA. Pathology, diagnostics, and classification of medulloblastoma. Brain Pathol. 2020;30(3):664-78.
31. Burger PC, Scheithauer BW. Medulloblastoma. In: Burger PC, editor. Diagnostic Pathology: Neuropathology. Salt Lake City: Amirsys; [year unknown]. p. 220-33.
32. Yachnis AT, Perry A. Embryonal (Primitive) Neoplasms of the Central Nervous System. In: Perry A, Brat DJ, editors. Practical Surgical Neuropathology: A Diagnostic Approach. Philadelphia: Churchill Livingstone; 2010. p. 165-84.
33. Korshunov A, Chavez L, Northcott PA, Sharma T, Ryzhova M, Jones DTW, et al. DNA-methylation profiling discloses significant advantages over NanoString method for molecular classification of medulloblastoma. Acta Neuropathol. 2017;134(6):965-7.
34. Zhang Y, Chen F, Donehower LA, Scheurer ME, Creighton CJ. A pediatric brain tumor atlas of genes deregulated by somatic genomic rearrangement. Nat Commun. 2021;12(1):937.
35. DeSisto J, Lucas JT Jr, Xu K, Donson A, Lin T, Sanford B, et al. Comprehensive molecular characterization of pediatric radiation-induced high-grade glioma. Nat Commun. 2021;12(1):5531.
36. Ellison DW, Figarella-Branger D, Pfister SM, von Deimling A, Wesseling P. Embryonal Tumours. In: WHO Classification of Tumours Editorial Board, editor. Central Nervous System Tumours. 5th ed. Lyon: IRAC; 2021. p. 200-19. (WHO Classification of Tumours; vol. 6).
37. Tanboon J, Williams EA, Louis DN. The Diagnostic Use of Immunohistochemical Surrogates for Signature Molecular Genetic Alterations in Gliomas. J Neuropathol Exp Neurol. 2016;75(1):4-18.